



Defining an NK Cell-enriched Rejection-like Phenotype in Liver Transplant Biopsies From the INTERLIVER Study

Katelynn S. Madill-Thomsen, PhD,¹ Patrick T. Gauthier, PhD,¹ Marwan Abouljoud, MD,² Chandra Bhati, MD,³ David Bruno, MD,⁴ Michał Ciszek, MD, PhD,⁵ Magdalena Durlik, MD,⁶ Sandy Feng, MD, PhD,⁷ Bartosz Foroncewicz, MD, PhD,⁵ Michał Grąt, MD, PhD,⁸ Krzysztof Jurczyk, MD, PhD,⁹ Josh Levitsky, MD,¹⁰ Geoff McCaughan, MD, PhD,¹¹ Daniel Maluf, MD,⁴ Aldo Montano-Loza, MD, PhD,¹² Dilip Moonka, MD,² Krzysztof Mucha, MD, PhD,⁵ Marek Myślak, MD, PhD,⁹ Agnieszka Perkowska-Ptasińska, MD, PhD,¹³ Grzegorz Piecha, MD,¹⁴ Trevor Reichman, MD,³ Olga Tronina, MD, PhD,⁸ Marta Wawrzynowicz-Syczewska, MD, PhD,⁹ Samir Zeair, MD, PhD,⁹ and Philip F. Halloran, MD, PhD¹

Background. Initial analysis of liver transplant biopsies in the INTERLIVER study (ClinicalTrials.gov; unique identifier NCT03193151) using rejection-associated transcripts failed to find an antibody-mediated rejection state (ie, rich in natural killer [NK] cells and with interferon-gamma effects). We recently developed an optimization strategy in lung transplants that isolated an NK cell-enriched rejection-like (NKRL) state that was molecularly distinct from T cell-mediated rejection (TCMR). Here we apply the same strategy to a liver transplant biopsy population. **Methods.** We used this strategy to search for a molecular NKRL state in 765 consented liver transplant biopsies collected at participating international centers for gold-standard histology and molecular assessment by genome-wide microarrays. Validation through a training set-test set approach of an optimized selection of variables as inputs into unsupervised rejection classification identified an NKRL state in livers. **Results.** The full model classified 765 biopsies into the following molecular phenotypes, characterized by their gene expression: no-rejection 54%, TCMR 16%, NKRL 13%, and injury 16%. Top TCMR transcripts were expressed in effector T cells; top NKRL transcripts were almost exclusively expressed in NK cells; and both had increased interferon- γ -inducible transcripts, which were more pronounced in TCMR. Most TCMR biopsies had significant parenchymal injury, molecular fibrosis, and abnormal biochemistry. NKRL biopsies had no excess of injury, fibrosis, or biochemistry abnormalities. **Conclusions.** Optimized rejection algorithms indicate that some liver transplants manifest an NKRL state that is well tolerated in the short term postbiopsy and with minimal injury and relatively normal biochemistry, while also underscoring the potential of TCMR to produce extensive parenchymal injury.

(Transplantation 2025;109: 1367–1382).

Received 10 April 2024. Revision received 31 July 2024.

Accepted 13 August 2024.

¹ Alberta Transplant Applied Genomics Centre, Edmonton, AB, Canada.

² Henry Ford Hospital, Detroit, MI.

³ Department of Surgery, Virginia Commonwealth University, Richmond, VA.

⁴ Department of Surgery, University of Maryland, Baltimore, MD.

⁵ Department of Immunology, Transplantology and Internal Diseases, Medical University of Warsaw, Warsaw, Poland.

⁶ Department of Transplant Medicine, Nephrology and Internal Diseases, Medical University of Warsaw, Warsaw, Poland.

⁷ Department of Surgery, University of California San Francisco, San Francisco, CA.

⁸ Department of General, Transplant and Liver Surgery, Medical University of Warsaw, Warsaw, Poland.

⁹ Department of Infectious Diseases, Hepatology and Liver Transplantation, Pomeranian Medical University, Szczecin, Poland.

¹⁰ Department of Medicine, Northwestern University, Chicago, IL.

¹¹ Australian National Liver Transplant Unit, Centenary Research Institute, Royal Prince Alfred Hospital, University of Sydney, Sydney, NSW, Australia.

¹² Department of Medicine, University of Alberta, Edmonton, AB, Canada.

¹³ Department of Pathology, Medical University of Warsaw, Warsaw, Poland.

¹⁴ Department of Nephrology, Transplantation and Internal Medicine, Medical University of Silesia, Katowice, Poland.

This research has been principally supported by grants from Genome Canada, Canada Foundation for Innovation, the University of Alberta Hospital Foundation, the Alberta Ministry of Advanced Education and Technology, the Mendez National Institute of Transplantation Foundation, and the Industrial Research Assistance Program. Partial support was also provided by funding from a licensing agreement with the One Lambda division of Thermo Fisher Scientific. P.F.H. held a Canada Research Chair in Transplant Immunology until 2008 and currently holds the Muttart Chair in Clinical Immunology.

P.F.H. holds shares in Transcriptome Sciences Inc, a University of Alberta research company dedicated to developing molecular diagnostics, supported in part by a licensing agreement between TSI and Thermo Fisher Scientific and by a research grant from Natera Inc. P.F.H. is a consultant to Natera Inc and Argenx BV. The other authors declare no conflicts of interest.

K.M.T. and P.G. were responsible for data analysis and interpretation, as well as writing, editing, and reviewing the article. P.F.H. was the principal investigator, edited and reviewed the article, and was responsible for data interpretation and study design. M.A., C.B., D.B., M.C., M.D., S.F., B.F., M.G., K.J., J.L., G.M., D.M., A.M.L., D.M., K.M., M.M., A.P.P., G.P., T.R., O.T., M.W.S., and S.Z. all contributed biopsies and accompanying phenotype data to the study.

The CEL files are available on the Gene Expression Omnibus website (GSE277334).

ClinicalTrials.gov: unique identifier NCT03193151

INTRODUCTION

Rejection assessment in liver transplantation remains an important issue, particularly as it relates to optimal immunosuppression management and preventing graft loss.¹⁻⁵ The current standard of care for rejection diagnoses is liver biopsy assessed by Banff histology,⁶ which yields a reported incidence of T cell-mediated rejection (TCMR) in the first year of 10%–30% with some interobserver variation,⁷⁻¹³ whereas late TCMR is rare. Liver transplants are immunologically unique and are thought to tolerate TCMR relatively well, inviting clinicians to consider reducing immunosuppression but with uncertainty about the risks versus benefits,¹⁴⁻¹⁸ that is, inadequate treatment of TCMR may lead to chronic rejection.¹³ Liver function biochemistry abnormalities are associated with but not specific to TCMR versus other causes of functional abnormalities (eg, steatohepatitis),^{19,20} and evidence of chronic graft injury has been found in liver transplant biopsy populations with normal biochemistry and stable function.²¹ Antibody-mediated rejection (AMR) in liver transplants (prevalence speculated at <1% for acute AMR¹³) remains a controversial phenotype,^{6,16,22-24} and the lack of routine donor-specific antibody (DSA) testing across all centers presents an additional challenge.

Assessment of liver rejection presents an opportunity to apply precise and quantitative molecular approaches.²⁵⁻²⁹ Previous analysis of liver transplant biopsies in the INTERLIVER study (ClinicalTrials.gov; unique identifier NCT03193151) using the Molecular Microscope Diagnostic System (MMDx) identified a molecular TCMR state but found no AMR-like phenotype similar to that seen in heart and kidney transplants³⁰—that is, enriched in natural killer (NK) cells and with increased interferon-gamma (IFN- γ) effects. This suggested that molecular AMR in livers is either rare or has a different phenotype than in hearts and kidneys, consistent with the complex perspectives on liver AMR in the literature.^{6,22,31-36} We followed this initial rejection analysis with a molecular assessment of liver parenchymal injury, focusing on steatohepatitis and fibrosis.³⁷ Recently, the role of NK cells in kidney AMR was supported by the felzartamab study (ClinicalTrials.gov; unique identifier NCT05021484), which showed that depleting NK cells can suppress AMR activity,³⁸ but liver NK cells may have other roles not seen in kidney transplants.³⁹⁻⁴²

The present study aimed to reexamine the question of gene expression associated with an NK cell-enriched molecular phenotype, using a recently developed optimization approach to transplant rejection assessment.⁴³ An optimal model was selected for its separation of molecular AMR-like

and TCMR-like activity along principal component 2 (PC2) and validated by developing the model in a training set and observing the fit in a test set. The full model was used in 765 prospectively collected liver transplant biopsies from the INTERLIVER study to search for an NK cell-enriched rejection-like (NKRL) state based on gene expression. We separated liver biopsies having TCMR and AMR gene expression profiles (using classifiers originally derived in kidney transplants), but this does not mean that the NK-rich state in the liver will necessarily be AMR-related. The goal was to assign rejection classes, establish the molecular features unique to these classes, and assess the relationships between molecular rejection and injury phenotypes.

The Consolidated Standards of Reporting Trials diagram and study design are shown in Figure 1A and B, respectively.

MATERIALS AND METHODS

Population and Demographics

We examined 765 biopsies prospectively collected from 680 consented (per local standards and IRB approval at each participating center) liver transplant patients in 15 international centers during the INTERLIVER study (Table S1, SDC, <http://links.lww.com/TP/D210>). All biopsies were stabilized in RNALater and shipped to the lab facility for analysis per established protocols.⁴⁴ Subsets of this biopsy population ($N = 337$ and $N = 235$) were used in prior publications.^{30,37} Additional data or biopsy collection details are provided in Supplemental Methods (SDC, <http://links.lww.com/TP/D209>).

Microarray Analysis

Total RNA was extracted from all biopsies and processed following INTERLIVER methods used previously.⁴⁴⁻⁴⁶ The CEL files are available on the Gene Expression Omnibus website (GSE277334). Two CEL files were excluded from the GEO upload due to duplication.

Rejection and Injury-associated Transcript Sets

Transcript sets associated with biological mechanisms in rejection and injury were previously annotated⁴⁷ (<https://www.ualberta.ca/medicine/institutes-centres-groups/atagc/research/gene-lists>; Table S2, SDC, <http://links.lww.com/TP/D211>).

New transcript sets were generated using the top 20 transcripts from a selection of previously defined rejection-associated classifier scores: AMR (AMR_{Prob}), glomerulitis ($g>0_{Prob}$), peritubular capillaritis ($ptc>0_{Prob}$), TCMR ($TCMR_{Prob}$), tubulitis ($t>1_{Prob}$), and interstitial infiltrate ($i>1_{Prob}$) classifiers.⁴³

All transcript set values represent the mean fold change in expression compared with a control group (defined as biopsies with archetype scores rejection archetype no-rejection score >0.7 and injury archetype normal score >0.7).

Optimization of Transcript Set Combinations for Liver Rejection Models

We optimized the selection from 14 potential transcript sets as inputs (AMR-associated transcripts [AMR-RAT], TCMR-associated transcripts [TCMR-RAT],

Visual abstract is available online at doi.org/10.1097/TP.00000000000005269.

Supplemental digital content (SDC) is available for this article. Direct URL citations appear in the printed text, and links to the digital files are provided in the HTML text of this article on the journal's Web site (www.transplantjournal.com).

Correspondence: Philip F. Halloran, MD, PhD, Alberta Transplant Applied Genomics Centre, #250 Heritage Medical Research Centre, University of Alberta, Edmonton, AB T6G 2S2, Canada. (phallora@ualberta.ca).

Copyright © 2025 The Author(s). Published by Wolters Kluwer Health, Inc. This is an open-access article distributed under the terms of the Creative Commons Attribution-Non Commercial-No Derivatives License 4.0 (CCBY-NC-ND), where it is permissible to download and share the work provided it is properly cited. The work cannot be changed in any way or used commercially without permission from the journal.

ISSN: 0041-1337/20/1098-1367

DOI: 10.1097/TP.00000000000005269

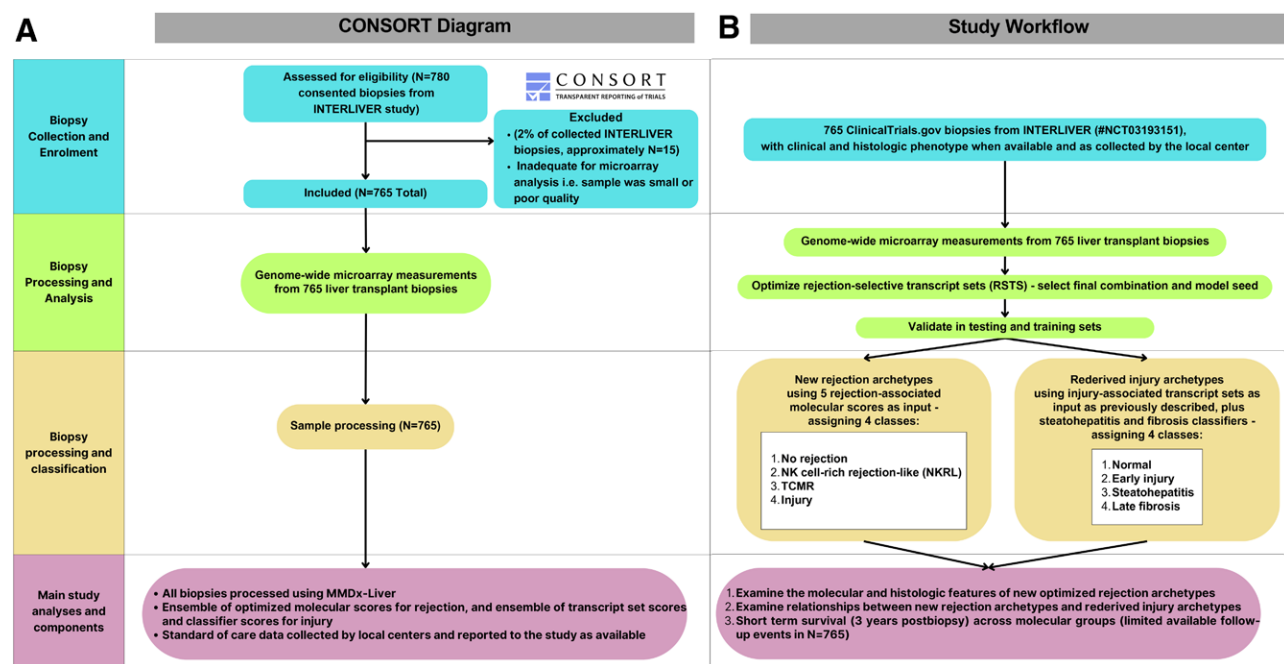


FIGURE 1. Study flowcharts for these analyses. A, CONSORT diagram. B, Study design. CONSORT, Consolidated Standards of Reporting Trials; MMDx, Molecular Microscope Diagnostic System; NKRL, natural killer cell–enriched rejection-like; TCMR, T cell–mediated rejection.

all-rejection-associated transcripts [Rej-RAT], interferon gamma and rejection-induced transcripts 1 [GRIT1], T-cell burden [TCB], NK cell burden [NKB], quantitative cytotoxic T cell–associated transcripts [QCAT], DSA-selective transcript [DSAST], AMR_{Prob} , $\text{g}>0_{\text{Prob}}$, $\text{ptc}>0_{\text{Prob}}$, $\text{TCMR}_{\text{Prob}}$, $\text{t}>1_{\text{Prob}}$, and $\text{i}>1_{\text{Prob}}$ scores). PC analyses (PCAs) were done using all possible combinations of transcript sets (excluding combinations with <5 inputs; $N = 14913$), and Spearman correlation coefficients (SCCs) were used to assess the maximal separation in PC2 (ie, the dimension separating AMR and TCMR in heart and kidney transplant populations) between biopsies with elevated AMR_{Prob} and those with elevated $\text{TCMR}_{\text{Prob}}$ ⁴³ (Figure 2). Combinations with PC2 SCC <0.25 for AMR_{Prob} or $\text{TCMR}_{\text{Prob}}$ and/or in the same direction were excluded (ie, PC2 SCCs for AMR_{Prob} and $\text{TCMR}_{\text{Prob}}$ had to be opposing). The final combination was selected on the basis of the highest summed rank of PC2 SCC for AMR_{Prob} and $\text{TCMR}_{\text{Prob}}$. The optimization process was validated by developing PCA and archetype models in a training set of 382 biopsies. Biopsies were assigned randomly to the training and test sets. Training set algorithms then classified a test set of 383 biopsies, with agreement evaluated in terms of archetypal groupings and top genes associated with TCMR and NKRL states in training and test sets. A final combination of 5 transcript sets (AMR_{Prob} and $\text{TCMR}_{\text{Prob}}$ transcript set scores, NKB, TCB, and AMR-RATs) was selected on the basis of optimization in 765 liver biopsies.

Archetypal Analysis

Archetypal analysis is a clustering method that identifies (n) theoretical idealized extreme phenotypes called archetypes and assigns each biopsy n scores relating to each archetype. By convention, biopsies are assigned to archetype clusters based on their highest archetype score. The scree plot “elbow method” plus knowledge of clinical liver phenotypes and previous experience^{30,48,49} determined the appropriate number of groups. Archetypal analysis was

performed using the “archetypes” package,⁵⁰ as previously described.^{30,37}

We updated our previous 337 liver transplant injury model³⁷ using the same input transcript set scores: alternative macrophage activation-associated transcripts 1 (AMAT1),⁵¹ damage-associated molecular pattern transcripts (DAMP),⁵² immunoglobulin transcripts (IGT),⁵³ injury and repair-induced transcripts-day 3 (IRIT3),⁵⁴ injury and repair-induced transcripts-day 5 (IRIT5),⁵⁴ quantitative constitutive macrophage-associated transcripts (QC MAT),⁵⁵ plus previously developed steatohepatitis and fibrosis classifier scores.³⁷

Dimensionality Reduction and Data Visualization

PCA was used to reduce the dimensionality of the data set, facilitating analysis and visualization of the data in R⁵⁶ using the “FactoMineR” package⁵⁷ and selected transcript sets as input. To depict the activity of molecular AMR and TCMR in relationship to the developed models, contours of AMR_{Prob} and $\text{TCMR}_{\text{Prob}}$ transcript set scores were derived using generalized additive models using the “mgcv” package⁵⁸ in R and visualized as a grid overlaid on PCA plots.

Cellular Expression

Cellular expression per gene was assessed per dominant expression in a cell panel⁵⁹ or using Human Protein Atlas.⁶⁰

Time Course Analyses

Prevalence of archetype groupings over time posttransplant was represented by restricted cubic splines using logistic regression and the “rcs”⁶¹ function in R.

Random Forests

Random forests were generated using “rfsrc”.⁶² Event data were death censored within 3 y postbiopsy.

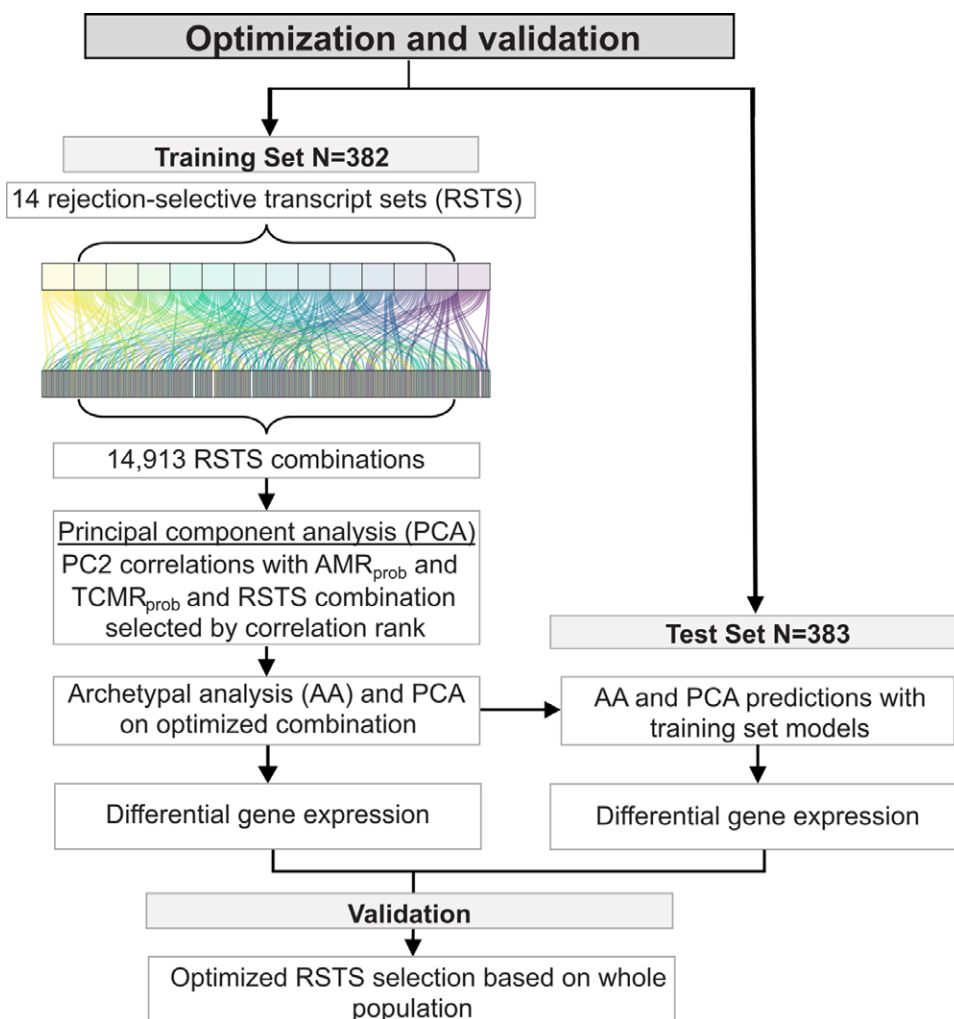


FIGURE 2. Optimization strategy and validation. The data set was split into a training and test set ($N = 382$ and $N = 383$, respectively). Optimization began with 14 potential rejection-selective transcript sets: 6 kidney classifier transcript sets (derived from a t test for the classifiers AMR_{Prob} , $\text{TCMR}_{\text{Prob}}$, $g > 0$, $\text{ptc} > 0$, $t > 1$, $i > 1$, and using 20 probe sets each) and 8 transcript sets: AMR-RAT, TCMR-RAT, Rej-RAT, GRIT1, TCB, NKB, QCAT, DSAST; IQR filtered (766 probe sets). PCAs were applied to all 14913 possible transcript set combinations. Combinations were then ranked on the basis of the resulting SCCs for AMR_{Prob} and $\text{TCMR}_{\text{Prob}}$ transcript set scores with PC2 (ie, AMR- and TCMR-activity along PC2). A single combination of transcript sets was chosen based on the lowest summed SCC rank. The resulting AA and PCA models obtained from the optimized transcript sets in the training set were then applied to test set, and agreement in AA classification and genes most associated with NKRL and TCMR was used to validate the approach. A final optimized model was derived in the entire population. AA, archetypal analysis; AMR, antibody-mediated rejection; AMR_{Prob} , AMR probability classifier; AMR-RAT, AMR-associated transcript; DSA, donor-specific antibody; DSAST, DSA-selective transcript; g , glomerulitis; GRIT, interferon gamma and rejection-induced transcript; i , interstitial infiltrate; IQR, interquartile range; NKB, natural killer cell burden; NKRL, NK cell-enriched rejection-like; PC, principal component; PCA, PC analysis; ptc, peritubular capillaritis; QCAT, quantitative cytotoxic T cell-associated transcript; Rej-RAT, all rejection-associated transcript; SCC, Spearman correlation coefficient; t , tubulitis; TCB, T-cell burden; TCMR, T cell-mediated rejection.

Differential Expression Analyses

Gene expression in 8287 interquartile range–filtered probe sets (range >0.5 across all 765 liver biopsies) among rejection and injury archetype groups were compared using the “limma” R package.^{63,64}

Comparison of Transcript Sets Across Archetypes

Differences in interquartile range–filtered transcript set scores among rejection and injury archetype groups were assessed using an aligned-rank transformed ANOVA⁶⁵ via the “ARTool” R package.⁶⁶

Gene Ontology Analysis

Overrepresentation analyses by gene ontology (GO) terms were performed with the top 300 nonunique genes sorted by

SCC for each archetype cluster using the “enrichGO”⁶⁷ function in R. The top 10 terms were selected by descending SCC (only 9 terms available for the injury group).

RESULTS

Study Population and Demographics

We analyzed 765 prospectively collected INTERLIVER biopsies from 680 patients, mainly for indications (Table 1). The median time posttransplant was 894 d (range, 0–12 569 d). The median follow-up time was 89 d. DSA testing per center practice was only performed for 163 biopsies (86/163 DSA positive). Biochemistry measurements are summarized in Table S3 (SDC, <http://links.lww.com/TP/D212>).

TABLE 1.
INTERLIVER patient and biopsy characteristics

Characteristics	Value					
Patient characteristics (N = 680)						
Recipient sex (% total)						
Male	393 (53%)					
Female	355 (47%)					
Not recorded	17					
Recipient age at transplant (median, range)	49 (0–73)					
Donor age at transplant (median, range)	39 (1–86)					
Primary disease (% total) ^a						
Alcoholic liver disease	44					
Autoimmune hepatitis	48					
Hepatitis B	41					
Hepatitis C	88					
Hepatocellular carcinoma	68					
Nonalcoholic steatohepatitis	49					
Primary biliary cholangitis	32					
Primary sclerosing cholangitis	63					
Nonalcoholic fatty liver disease	6					
Cirrhosis ^b	198					
Other	105					
Not recorded	106					
Biopsy characteristics (N = 765)						
Days from transplant to biopsy, median (mean, range)	894 (1852, 0–12569)					
Days to most recent follow-up after biopsy (415 NA), median (mean, range)	89 (298, 0–3732)					
Immunosuppression at biopsy (% total) ^a						
Corticosteroids	110					
Cyclosporine	30					
Tacrolimus	364					
Other	120					
None	12					
Not recorded	336					
Indication for biopsy (% total)						
For cause	539 (70%)					
Protocol/surveillance	125 (16%)					
Not recorded	101 (13%)					
DSA at biopsy (N = 163/765 biopsies with available DSA result)	Number of results (% of all biopsies)					
Positive	86 (11%)					
Negative	77 (10%)					
Not tested/data not available	602 (79%)					
Histology feature	Grades (biopsy count per grade)					
Steatohepatitis	0 417	1 60	2 19	3 8	Not recorded 261	
Fibrosis	None (0) 253	Mild (1) 164	Moderate (2) 58	Severe (3) 21	Cirrhosis (4) 9	Not recorded 260

Missing DSA values included those not provided by the center, or instances where the test was not done within a relevant time period of the biopsy (± 7 d). Sixteen biopsies had steatohepatitis grades >0 and fibrosis grades >1 simultaneously.

^aSome patients fell under multiple categories.

^bIncludes "alcoholic cirrhosis."

DSA, donor-specific antibody; NA, not available or not done.

Optimization Strategy and Validation

The optimization selected AMR_{Prob} and TCMR_{Prob} classifier-based transcript sets, AMR-RAT, NKB, and TCB, as input. Archetypal classification in the training set (N = 382; Figure 3A and B) was used to classify the test set (N = 383; Figure 3C and D). Archetypal classification assigned 4 groups, that is, molecular phenotypes named for their dominant molecular features: no-rejection (NR), NKRL, TCMR, and injury (features discussed in more detail below).

Test set classes were similar to the training set, satisfying validation concerns. In particular, top genes in the test set versus the training set were very similar in terms of fold change in NKRL versus NR, mean expression in the NKRL biopsies, fold change rank, and P value (false discovery rate) rank (Table S4, SDC, <http://links.lww.com/TP/D213>). The top genes in TCMR versus NR (Table S5, SDC, <http://links.lww.com/TP/D214>) were similar in the test set versus the training set.

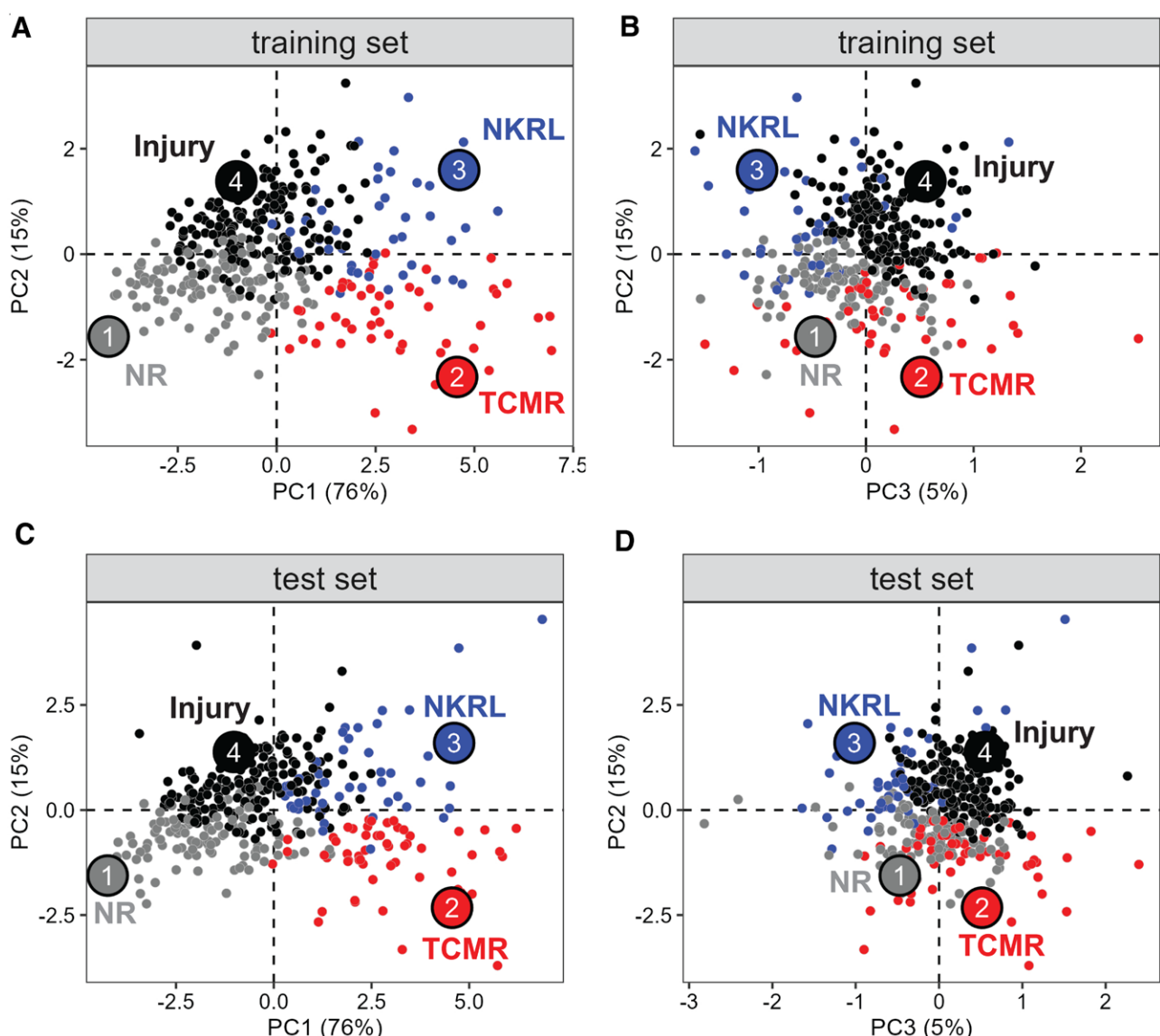


FIGURE 3. Validation of PCA and AA using the optimization strategy for selection rejection-selective transcript sets. The optimal combination was defined by summed rank of SCCs for AMR_{Prob} and $\text{TCMR}_{\text{Prob}}$ transcript set scores with PC2 (ie, AMR- and TCMR-activity along PC2). The optimized PCA and AA classification derived in the training set are shown in PC2 vs PC1 (A) and PC2 vs PC3 (B). The training set PCA and AA models were then applied to test set and are shown in PC2 vs PC1 (C) and PC2 vs PC3 (D). AA, archetypal analysis; AMR, antibody-mediated rejection; AMR_{Prob} , AMR probability classifier; NKRL, natural killer cell-enriched rejection-like; NR, no rejection; PC, principal component; PCA, PC analysis; SCC, Spearman correlation coefficient; TCMR, T cell-mediated rejection; $\text{TCMR}_{\text{Prob}}$, TCMR probability classifier.

Final PC and Archetypal Analysis

Having validated the optimized model, the selected combination of 5 transcript sets was applied to all 765 biopsies to create the final 4-archetype model. All transcript sets were positively correlated with PC1 (ie, all-rejection; Figure 4A). NKB and DSAST transcript sets had the highest positive PC2 correlation compared with other transcript sets. Thus, PC2 discriminated biopsies with high NKB and DSAST scores from those with high expression of TCMR-specific transcript set scores (Figure 4B). Time of biopsy posttransplant correlated positively with PC2. Transcript set SCCs with PC3 discriminated AMR-related features from TCMR-related features, but the total variance explained by PC3 was small (5%).

Resulting archetype groups were interpreted according to molecular associations (Figure 4C and D): NR

($N = 416$; 54%), TCMR ($N = 125$; 16%), NKRL ($N = 98$; 13%), and Injury ($N = 126$; 16%). NKRL and TCMR separated from injury and NR in PC1. NKRL separated from TCMR in PC2 and PC3. Contour plots indicated that AMR activity was generally highest in the region populated by biopsies classified as NKRL, and TCMR activity was generally higher in the region populated by biopsies classified as TCMR (Figure 4E and F).

Top Transcripts Correlating With Each Archetype Score

Transcripts most strongly correlated with the NR score were annotated as expressed in normal livers (eg, SLC47A1, USP30; Table 2). Transcripts correlated with TCMR were related to T-cell activity, for example, the T-cell alpha and beta receptors (TRAC and TRBC1) and

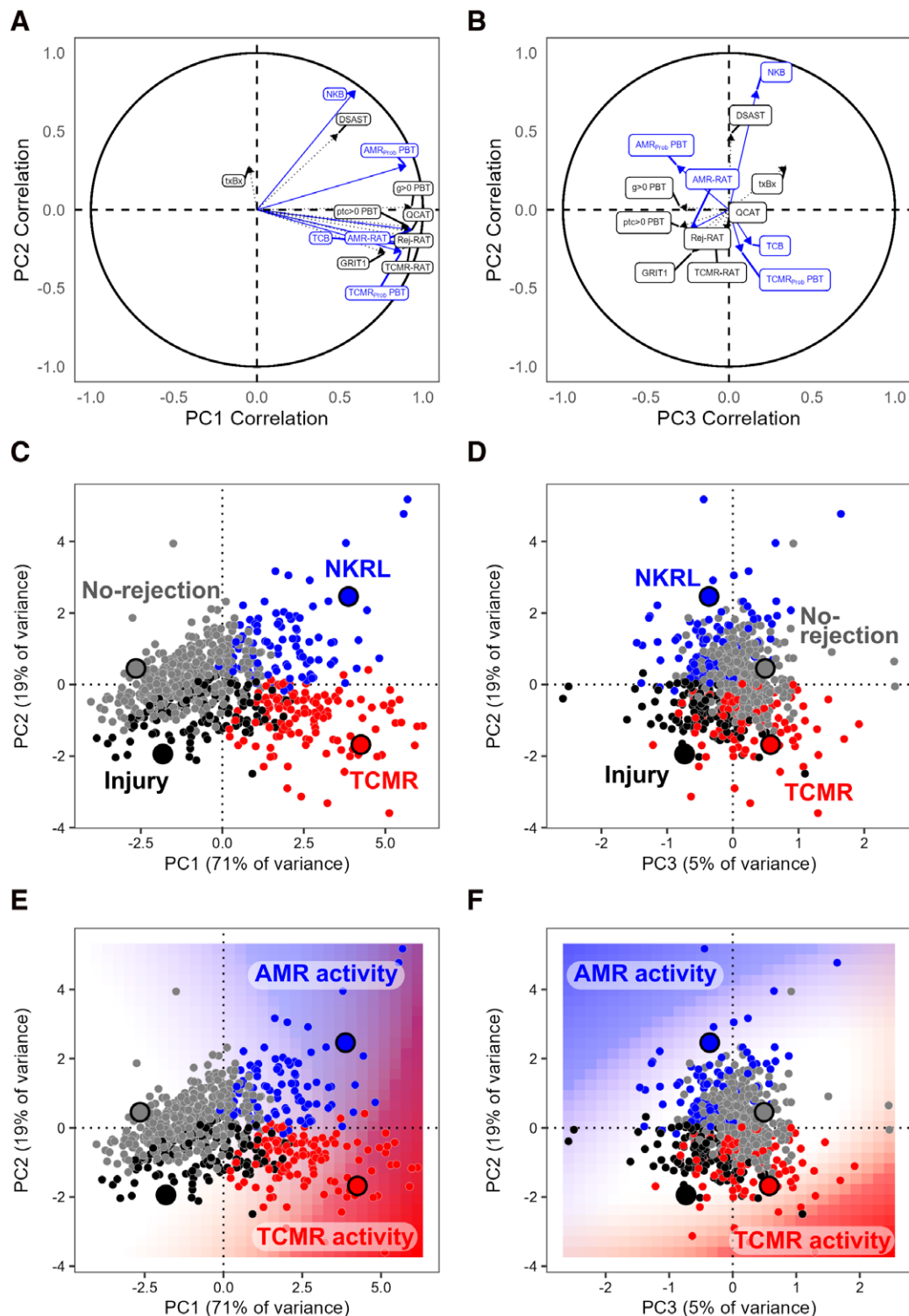


FIGURE 4. A and B, Factor maps for the PC analysis. Blue solid lines indicate the input variables, whereas black dotted lines indicate other rejection-related transcript sets considered for input during the optimization process, as well as time of biopsy posttransplant (TxBx). Visualization of the population of 765 liver biopsies shows an NKRL phenotype, TCMR phenotype, injury (no rejection), and no rejection (with minimal injury) in PC2 vs PC1 (C) and PC2 vs PC3 (D). Contour plots depict the degree of overlap in AMR_{Prob} and TCMR_{Prob} transcript set scores (ie, AMR and TCMR activity) with respect to biopsy classification in PC2 vs PC1 (E) and PC2 vs PC3 (F). We note that the published name for AMR_{Prob} is "ABMR_{Prob}" however we have adjusted the name per preferred journal style. AMR, antibody-mediated rejection; AMR_{Prob}, AMR probability classifier; DSAST, donor-specific antibody-selective transcript; GRIT, interferon gamma and rejection-induced transcript; NKB, natural killer cell burden; NKRL, NK cell-enriched rejection-like; PC, principal component; QCAT, quantitative cytotoxic T cell-associated transcript; TCB, T-cell burden; TCMR, T cell-mediated rejection; TCMR_{Prob}, TCMR probability classifier; TCMR-RAT, TCMR-associated transcript; TxBx, time of biopsy posttransplant.

TABLE 2.

Top 10 (by correlation coefficient) nonredundant transcripts positively correlating with archetype scores in 765 liver biopsies

No-rejection score		TCMR score	
Gene symbol	Annotation ^a	Gene symbol	Annotation ^a
SLC47A1	parenchyma	TRAC	T cell, TCMR-RAT ^b
USP30	parenchyma	TRBC1	T cell, TCMR-RAT
CDNF	parenchyma	TRBC2	T cell, TCMR-RAT
GREB1L	parenchyma	IL23A	T cell, TCMR-RAT
THRBL	parenchyma	CD3D	T cell, TCMR-RAT
DNAJC25	parenchyma	CD2	T cell, TCMR-RAT
PAIP2B	parenchyma	CD27	T cell, TCMR-RAT
ALAD	parenchyma	CD8A	T cell, TCMR-RAT
BCKDHB	parenchyma	LCK	T cell, TCMR-RAT
ZNF395	parenchyma	CLEC2D	T cell, TCMR-RAT

NKRL score		Injury score	
Gene symbol ^c	Annotation ^a	Gene symbol	Annotation ^a
KLRF1	NK cell, AMR-RAT ^b	EGLN1	Injury induced
SH2D1B	NK cell, AMR-RAT	CST3	Injury induced
GNLY	NK cell, AMR-RAT	TMBIM1	Injury induced
TRDC	NK cell, AMR-RAT	SLPI	Injury induced
CD160	NK cell, AMR-RAT	PVR	Injury induced
FGFBP2	NK cell, AMR-RAT	TMRRSS2	Injury induced
IL2RB	NK cell, T cell	KRT8	Injury induced
PRF1	NK cell, T cell	DUSP3	Injury induced
CX3CR1	NK cell, AMR-RAT	RIPK4	Injury induced
KLRD1	NK cell, T cell	UBIAD1	Injury induced

^aBased on literature and expression in a cell panel or injury induced in kidney transplants or experimental models.

^bTCMR-RAT or AMR-RAT indicates transcripts with previous annotation as highly associated with TCMR or AMR, respectively, in kidney transplants.

^cIn a comparison of expression between NKRL and NR; CD160 ($F_C_{NKRLvsNR} = 1.6$, FDR = 5E-20), IL2RB ($F_C_{NKRLvsNR} = 1.6$, FDR = 9E-31), SH2D1A ($F_C_{NKRLvsNR} = 1.5$, FDR = 1E-34), CD27 ($F_C_{NKRLvsNR} = 1.4$, FDR = 3E-21), EOMES ($F_C_{NKRLvsNR} = 1.87$, FDR = 5E-28), and CXCR6 ($F_C_{NKRLvsNR} = 1.62$, FDR = 5E-28). Note that expression of FCGR3A in NKRL ($F_C_{NKRLvsNR} = 1.62$, FDR = 2E-14) is lower compared with TCMR ($F_C_{TCMRvsNR} = 2.14$, FDR = 2E-49, $F_C_{NKRLvsTCMR} = 0.76$, FDR = 3E-5). AMR, antibody-mediated rejection; AMR-RAT, AMR-associated transcript; FC, fold change; FDR, false discovery rate; NK, natural killer; NKRL, NK cell-enriched rejection-like; NR, no rejection; TCMR, T cell-mediated rejection.

CD3D—all previously annotated as TCMR-associated in the kidney, and others were associated with rejection in the liver,²¹ for example, ITK and CD8A.

Top transcripts correlated with the NKRL archetype score were all highly expressed in NK cells (eg, SH2D1B, GNLY). Top transcripts associated with the Injury class were all annotated as injury-induced in kidney transplants (eg, EGLN1, SLPI).

Molecular Features Correlated With the Rejection Archetype Scores

NR biopsies were relatively normal compared with other archetype groups, with minimal rejection or injury scores.

Biopsies called TCMR had a molecular phenotype characterized by elevated TCMR- and all rejection-associated features (ie, molecular scores trained previously on TCMR diagnoses, TCMR/T-cell features, or features of all rejection, including IFN- γ effects, in organ transplants; Table 3), as well as elevated parenchymal injury-associated

scores, that is, IRIT and injury and repair response associated transcript (IRRAT) scores.

NKRL biopsies had elevated AMR-associated transcript set scores: the AMR_{Prob} classifier transcript set and NKB, rejection-associated transcript set scores (eg, GRIT, albeit lower than in TCMR), and lower molecular injury scores.

Injury archetype biopsies showed elevated parenchymal injury-associated features, that is, IRIT, IRRAT, and damage-associated molecular pattern (DAMP) transcript scores. Some rejection-related transcript set scores were mildly elevated in Injury compared with NR (eg, GRIT) but lower than in TCMR or NKRL biopsies.

The Injury rejection archetype was earliest posttransplant (mean 895 d), followed by TCMR (1751 d) and NKRL (1751 d). The NR archetype group had the longest mean time posttransplant, with 2332 d.

Histologic and Clinical Features Associated With the Molecular Archetype Groups

We examined correlations between the molecular archetype groups and histologic or clinical features as reported for those biopsies. The NR archetype score negatively correlated with TCMR-related histology features (eg, portal inflammation; Table 4). The TCMR archetype score was positively correlated with portal, bile duct, and venous inflammation. The NKRL archetype score had no strong correlations with histologic features (only a weak correlation with cholestasis, $P = 0.0004$), suggesting that this molecular phenotype is unique and not fully captured by the histology features we assessed. The Injury score had a strong negative correlation with time posttransplant, venous inflammation, and fibrosis.

Data related to DSA positivity in this population was very limited (available in only 163/765 biopsies); therefore, we were unable to establish a reliable relationship between DSA positivity and molecular archetype groups.

Relationships Between Archetype Scores and Liver Biochemistry

We visualized these relationships in a correlation plot (Figure 5; the strength and direction of the correlation determine the shade of the cell, and asterisks note correlations with significant P values <0.001). TCMR-related scores (TCMR archetype score, TCMR_{Prob}, and TCB transcript set scores) correlated with each other and with abnormal biochemistry (depressed albumin, increased bilirubin, aspartate aminotransferase, alanine transaminase, and alkaline phosphatase). NKRL-related scores (NKRL archetype score, and AMR_{Prob} and NKB transcript set scores) strongly correlated with each other but not with biochemistry abnormalities. NR correlated negatively with Injury, TCMR, and NKRL archetype scores and showed relatively normal biochemistry. Injury correlated positively with abnormal biochemistry but negatively with rejection-associated scores (eg, TCMR or NKRL archetype scores), indicating abnormalities not strongly associated with rejection episodes.

GO Analysis of Top 300 Nonunique Genes Correlated With Each Archetype Score

GO analysis found the top enriched pathway terms from Biological Process, Molecular Function, Cellular

TABLE 3.

Comparison of multigene scores among rejection archetype groupings in livers (N = 765)

Category	Variable (means, unless otherwise specified)	NR (N = 416)	TCMR (N = 125)	NKRL (N = 98)	Injury (N = 126)	FDR
TCMR-related	TxBx (means ± SE)	2332.20 ± 114.19 a	1289.94 ± 172.63 b	1751.12 ± 207.55 b	895.13 ± 113.97 c	1.5E-16
	TxBx (median ± IQR)	1667.00 ± 3353.75 a	497.00 ± 1610.25 b	696.50 ± 3029.75 b	287.00 ± 1133 c	1.5E-16
	TCB ^a	0.34 ± 0.02 a	1.89 ± 0.04 b	1.03 ± 0.04 c	0.54 ± 0.04 d	1.9E-119
	TCMR-RAT	0.22 ± 0.01 a	1.23 ± 0.03 b	0.76 ± 0.03 c	0.49 ± 0.03 d	2.3E-147
	QCAT	0.26 ± 0.01 a	1.34 ± 0.04 b	0.87 ± 0.03 c	0.45 ± 0.03 d	7.3E-132
All rejection-related	TCMR _{Prob} classifier	0.05 ± 0.01 a	0.74 ± 0.03 b	0.33 ± 0.02 c	0.18 ± 0.02 d	1.6E-122
	PBT ^a					
	GRIT1	0.26 ± 0.02 a	1.09 ± 0.03 b	0.71 ± 0.04 c	0.62 ± 0.03 c	1.4E-107
AMR-related	Rej-RAT	0.32 ± 0.02 a	1.42 ± 0.03 b	1.01 ± 0.03 c	0.70 ± 0.03 d	1.3E-142
	AMR-RAT ^{a,b}	0.27 ± 0.01 a	1.08 ± 0.02 b	0.83 ± 0.02 c	0.55 ± 0.03 d	2.0E-144
	NKB ^a	0.06 ± 0.01 a	0.11 ± 0.02 b	0.55 ± 0.04 c	-0.27 ± 0.02 d	1.3E-73
Macrophage-related	AMR _{Prob} classifier	0.11 ± 0.01 a	0.49 ± 0.02 b	0.64 ± 0.02 c	0.18 ± 0.02 d	7.4E-105
	QCMAT	0.21 ± 0.01 a	0.84 ± 0.03 b	0.58 ± 0.03 c	0.52 ± 0.02 d	1.1E-112
	AMAT1	0.29 ± 0.01 a	1.08 ± 0.03 b	0.68 ± 0.03 c	0.66 ± 0.03 c	2.8E-93
Atrophy fibrosis-related	IGT	0.28 ± 0.03 a	1.14 ± 0.07 b	0.53 ± 0.06 c	0.34 ± 0.06 a	1.9E-29
	BAT	0.09 ± 0.01 a	0.44 ± 0.02 b	0.23 ± 0.01 c	0.15 ± 0.01 d	2.2E-66
	Fibrosis classifier	0.17 ± 0.01 a	0.37 ± 0.02 b	0.17 ± 0.01 a	0.20 ± 0.02 a	1.3E-20
Recent injury-related	IRITD3	0.16 ± 0.01 a	0.44 ± 0.02 b	0.24 ± 0.01 c	0.38 ± 0.02 d	3.8E-55
	IRITD5	0.17 ± 0.01 a	0.58 ± 0.03 b	0.29 ± 0.02 c	0.35 ± 0.02 c	8.7E-62
	IRRAT30	0.25 ± 0.02 a	0.78 ± 0.04 b	0.56 ± 0.04 c	0.62 ± 0.05 c	1.4E-43
Expressed in normal parenchymal tissue	LVT1	-0.25 ± 0.02 a	-0.77 ± 0.04 b	-0.40 ± 0.03 c	-0.65 ± 0.04 d	6.9E-56
	LVT2	-0.21 ± 0.02 a	-0.70 ± 0.04 b	-0.38 ± 0.04 c	-0.58 ± 0.03 d	2.2E-51
Steatohepatitis	Steatohepatitis classifier	0.19 ± 0.01 ab	0.17 ± 0.02 ac	0.12 ± 0.02 b	0.23 ± 0.03 c	0.0005

Multigene scores are the mean fold change in expression for all probes vs the mean expression for all probes in the control set.

Groups sharing the same letters are not different from one another for that molecular score.

FDR denotes the overall significance by aligned rank-transformed ANOVA for each individual score. We note that the published names for AMR_{Prob} and AMR-RAT is "ABMR_{Prob}" and "ABMR-RAT," however we have adjusted the name per preferred journal style.^aDenotes input variables.

^aWhile AMR-RATs were developed in AMR cases, they in fact perform as an all-rejection transcript set and have been listed as such in this table.
 AMAT1, alternative macrophage activation transcripts 1; AMR, antibody-mediated rejection; AMR_{Prob}, AMR probability classifier; AMR-RAT, AMR-associated transcript; BAT, B cell-associated transcripts; FDR, false discovery rate; GRIT1, interferon gamma and rejection-induced transcripts 1; IGT, immunoglobulin transcripts; IQR, interquartile range; IRITD3, injury and repair-induced transcripts, day 3; IRITD5, IRIT day 5; IRRAT30, injury and repair response-associated transcripts; LVT1, normal liver parenchyma transcripts 1 – without solute carrier; LVT2, normal liver parenchyma transcripts 2 – solute carriers; NKB, natural killer cell burden; NKRL, NK cell-enriched rejection-like; NR, no rejection; QCAT, quantitative cytotoxic T cell-associated transcripts; QCMAT, quantitative constitutive macrophage-associated transcripts; Rej-RAT, all rejection-associated transcripts; TCB, T-cell burden; TCMR, T cell-mediated rejection; TxBx, time of biopsy posttransplant.

Compartment, and Kyoto Encyclopedia of Genes and Genomes libraries (Table 5).

Top pathway terms from NR transcripts showed mainly normal tissue function (eg, small molecule catabolic process). Top terms in TCMR showed T cell- and leukocyte-associated activity (eg, regulation of T-cell activation). Top terms in NKRL showed similarities with the TCMR analysis (ie, associated with "immune response"). Injury showed terms associated with tissue damage and cell death (eg, extrinsic apoptotic signaling pathway).

We examined the genes that were enriched in the top 10 NR, TCMR, NKRL, or Injury GO terms (Figure 6), using a cell line panel to assess the dominant cell type expression for each gene. In NR, genes enriched in GO terms were primarily expressed in the epithelium, that is, hepatocytes (Figure 6A). Genes enriched in the TCMR GO terms (Figure 6B) were mainly expressed in T cells. Conversely, genes enriched in NKRL GO terms (Figure 6C) were predominantly expressed in NK cells (eg, CD160, XCL1, KLRL1), some sharing expression with T cells (eg, LCP2,

PVRIG). Finally, genes enriched in Injury GO terms (Figure 6D; only 9 terms available) were mainly expressed in epithelial cells.

Assessing Parenchymal Injury in the Rejection Archetypes

We updated our liver parenchymal injury archetype model in this population of 765 liver transplant biopsies, assigning 4 groups based on their gene expression (Figure 7): Normal (N = 458), Early-injury (N = 103), Steatohepatitis (N = 114), and Late fibrosis (N = 90).

Time Course of Rejection and Injury States in Liver Biopsies

NR archetype scores steadily increased over time post-transplant (Figure 8A). TCMR archetype scores increased between 200 and 1000 d posttransplant, then steadily declined. NKRL archetype scores were distributed widely over time but were increased slightly both early post-transplant (<100 d) and later posttransplant (>600 d)

TABLE 4.

Spearman correlations between new optimized rejection PCA and molecular archetype scores and histologic features in liver biopsies (N = 765)

Histology features	No rejection	TCMR	NKRL	Injury
Time of biopsy posttransplant	0.29, P = 5.8E-16	-0.06, P = 0.1	0.07, P = 0.07	-0.35, P < 2E-16
Rejection-related				
Portal inflammation	-0.29, P = 1.4E-12	0.25, P = 1.4E-9	0.04, P = 0.32	0.02, P = 0.7
Bile duct inflammation	-0.11, P = 0.02	0.15, P = 0.002	0.05, P = 0.3	-0.1, P = 0.04
Venous inflammation	-0.19, P = 5.3E-6	0.22, P = 1.4E-7	0.1, P = 0.01	-0.12, P = 0.007
Chronic rejection-related				
Bile duct degeneration	-0.03, P = 0.5	0.03, P = 0.45	-0.09, P = 0.04	0.05, P = 0.27
Focal obliteration	-0.04, P = 0.3	0.08, P = 0.06	-0.07, P = 0.08	-0.01, P = 0.8
Cholestasis	-0.10, P = 0.02	0.05, P = 0.22	-0.15, P = 0.0004	0.17, P = 4.2E-5
Mural fibrosis	-0.04, P = 0.3	0.09, P = 0.04	-0.1, P = 0.02	0.04, P = 0.39
Other disease-related				
Autoimmune hepatitis	-0.12, P = 0.005	0.10, P = 0.01	-0.06, P = 0.16	-0.01, P = 0.8
Steatohepatitis	0.13, P = 0.002	-0.09, P = 0.04	-0.07, P = 0.13	0.05, P = 0.28
Fibrosis	0.08, P = 0.07	0.004, P = 0.9	0.003, P = 0.95	-0.16, P = 0.0003
Recurrent HCV ^a	-0.20, P = 3.3E-6	0.17, P = 7.9E-5	0.015, P = 0.7	0.03, P = 0.5
Suspected CMV hepatitis	-0.09, P = 0.03	0.13, P = 0.003	-0.03, P = 0.6	-0.04, P = 0.3

Clinical data are ordinal scores. Cells were shaded if the P value was <0.01; bold indicates SCC ≥ 2.0 or ≤ 2.0.

^aSeventy biopsies were listed as positive for recurrent HCV.

CMV, cytomegalovirus; NKRL, natural killer cell–enriched rejection-like; PCA, principal component analysis; SCC, Spearman correlation coefficient; TCMR, T cell–mediated rejection.

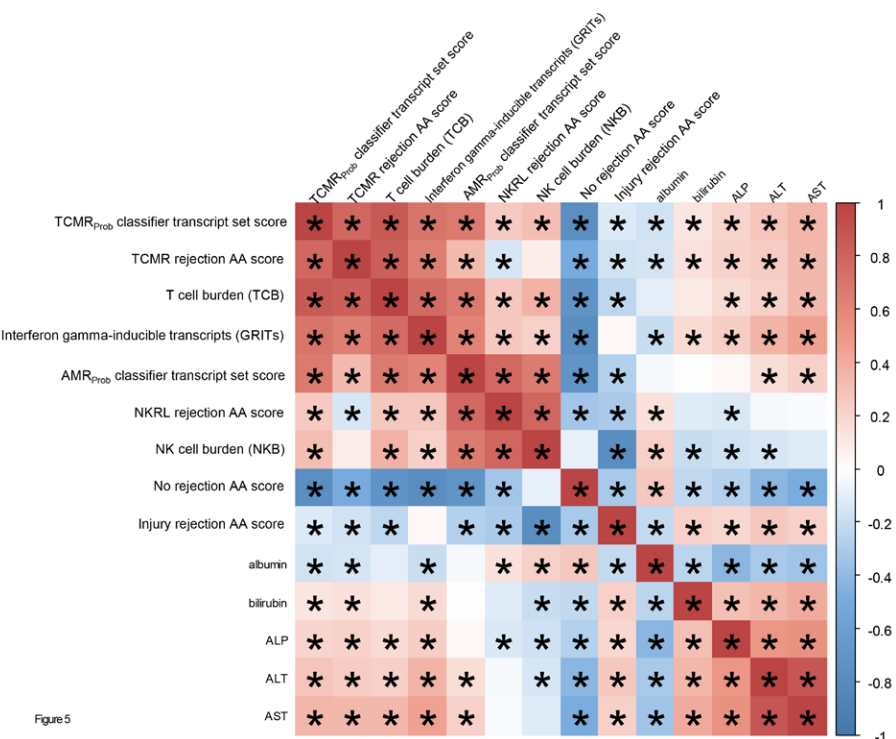


FIGURE 5. Correlation plot for rejection molecular features and standard of care biochemistry results. Positive correlations are shown as increasing red color in each cell, and negative correlations are shown as increasing blue color in each cell. Exact correlation-color matches are shown on the bar on the right-hand side of the chart. *A significant P value for that Spearman correlation (<0.001). AA, archetypal analysis; ALP, alkaline phosphatase; ALT, alanine transaminase; AMR, antibody-mediated rejection; AMR_{Prob}, AMR probability classifier; AST, aspartate aminotransferase; NKRL, natural killer cell–enriched rejection-like; TCMR, T cell–mediated rejection; TCMR_{Prob}, TCMR probability classifier.

and were more common than TCMR in the late period after 1000 d. Splines modeling the time course of rejection phenotypes for TCMR and NKRL had an inverse relationship, with NKRL peaking at approximately the same time posttransplant as TCMR is least common (300–400

d posttransplant). Injury scores were initially high and declined over time, likely reflecting recovery from the injury incurred during the donation-implantation process.

In comparison, among injury model archetype scores, Normal and Late fibrosis rose steadily over time

TABLE 5.

Top 10 GO terms using the top 300 nonunique genes sorted by correlation coefficient for each archetype cluster in 765 liver biopsies

No rejection		TCMR		NKRL		Injury ^a	
Term name	P	Term name	P	Term name	P	Term name	P
Small molecule catabolic process	4.74E-18	T-cell activation	5.67E-58	T-cell activation	4.02E-27	Extrinsic apoptotic signaling pathway	2.67E-07
Carboxylic acid catabolic process	1.04E-16	Lymphocyte differentiation	6.27E-40	Leukocyte-mediated immunity	2.46E-24	Regulation of apoptotic signaling pathway	4.87E-07
Organic acid catabolic process	1.51E-16	Regulation of T-cell activation	1.61E-38	Regulation of immune effector process	1.98E-22	Negative regulation of apoptotic signaling pathway	2.29E-06
Monocarboxylic acid catabolic process	1.39E-11	Mononuclear cell differentiation	2.93E-37	Immune response-regulating cell surface receptor signaling pathway	3.11E-22	Regulation of extrinsic apoptotic signaling pathway	2.49E-06
Cellular amino acid metabolic process	4.44E-11	Leukocyte cell-cell adhesion	3.4E-36	Activation of immune response	3.25E-22	Negative regulation of extrinsic apoptotic signaling pathway	5.12E-06
Mitochondrial matrix	1.64E-10	Regulation of leukocyte cell-cell adhesion	3.45E-34	Immune response-regulating signaling pathway	2.49E-21	Response to oxidative stress	8.92E-06
Fatty acid metabolic process	1.48E-09	T-cell differentiation	1.6E-33	Negative regulation of the immune system process	2.52E-21	Response to endoplasmic reticulum stress	9E-06
Cellular-modified amino acid metabolic process	4.5E-09	Positive regulation of leukocyte cell-cell adhesion	5.65E-32	Leukocyte cell-cell adhesion	2.92E-21	Biological process involved in a symbiotic interaction	3.11E-05
Alpha-amino acid metabolic process	7.2E-09	Positive regulation of T-cell activation	8.83E-31	Immune response-activating cell surface receptor signaling pathway	6.56E-21	Actin filament bundle organization	3.11E-05
Cellular amino acid catabolic process	1E-08	Positive regulation of leukocyte activation	1.57E-29	Immune response-activating signal transduction	6.56E-21		

Terms were searched from biological process, cellular component, molecular function, and Kyoto Encyclopedia of Genes and Genomes pathway libraries. All top pathways were from the biological process pathway library, with the exception of "mitochondrial matrix" in the no-rejection list, which was from the cellular component library.

^aOnly 9 terms were found for the Injury gene list.

GO, gene ontology; NKRL, natural killer cell-enriched rejection-like; TCMR, T cell-mediated rejection.

posttransplant, whereas Early-injury declined (Figure 8B). Steatohepatitis peaked around 400 d.

Rejection and Injury Variable Importance in Predicting 3-y Postbiopsy Graft Survival

We examined the importance of rejection and injury archetype scores for predicting 3-y postbiopsy (short term) survival in this population of 765 liver transplants using random forests (Figure 9). Due to limited follow-up, particularly the small number of failures ($N = 9$) reported in INTERLIVER, this estimate must be interpreted with caution and reexamined when longer follow-up is available. Nonetheless, the importance of variables in predicting graft loss was similar to results seen in kidney and heart transplants.⁶⁸⁻⁷² The most important variables predicting failure (2/3 top variables here) were related to injury rather than rejection (although at least some injury was due to TCMR). The TCMR archetype score was more important than the NKRL archetype score, consistent with biochemical abnormalities and parenchymal injury classes induced by TCMR. Hazard ratios (Table S6, SDC, <http://links.lww.com/TP/D215>) indicated that increased NR and Normal injury scores were protective (better survival), and increased TCMR

scores were detrimental (worse survival, other scores not interpretable due to insignificant P values).

DISCUSSION

These analyses identified an NKRL state in liver transplants that was different from TCMR and showed some similarities to the NK cell-enriched molecular AMR state in kidney and heart transplants (characterized by increased expression of NK cell and IFN- γ -inducible transcripts) and the NKRL state in lung transplants. Associated molecules and GO pathway analysis showed distinct TCMR-like and NK cell-enriched features in the TCMR and NKRL-like states, respectively. The NKRL state had a minimal molecular injury and biochemical abnormalities, whereas the TCMR state was associated with molecular injury, biochemical abnormalities, histologic inflammation, and molecular fibrosis classifier scores. NKRL seemed well tolerated in this observational cross-sectional short-term study: it had no strong correlations with histologic fibrosis, molecular fibrosis,³⁷ parenchymal injury classes, or abnormal biochemistry. However, we need to reserve judgment: AMR in kidney or heart transplants is also relatively well-tolerated short term with minimal parenchymal

T cells	Macrophages	NK cells	IFNG-inducible	Epithelial (Hepatocytes, others)					
A Genes that appear in top ten NR archetype GO terms (enriched in NR AA phenotype) N=765									
Term 1: small molecule catabolic process	Term 2: carboxylic acid catabolic process	Term 3: organic acid catabolic process	Term 4: monocarboxylic acid catabolic process	Term 5: cellular amino acid metabolic process	Term 6: mitochondrial matrix	Term 7: fatty acid metabolic process	Term 8: cellular modified amino acid metabolic process	Term 9: alpha-amino acid metabolic process	Term 10: cellular amino acid catabolic process
BCKDHB	BCKDHB	BCKDHB	CYP4A11	BCKDHB	BCKDHB	ACSM3	ALDH7A1	AMT	BCKDHB
AMT	AMT	AMT	CRAT	AMT	ACSM3	CBR4	IYD	IYD	AMT
CYP4A11	CYP4A11	CYP4A11	ABHD1	IYD	AMT	SLC27A5	CRAT	ALDH5A1	ALDH5A1
CRAT	CRAT	CRAT	ACACB	ALDH5A1	ALDH7A1	CYP4A11	GSTA1	ACADSB	ACADSB
ALDH5A1	ALDH5A1	ALDH5A1	XYLB	ACADSB	SIRT3	CRAT	SARDH	SLC25A13	SARDH
ACADSB	ACADSB	ACADSB	LDHD	SLC25A13	CBR4	ACADSB	SLC46A1	SARDH	IVD
ABHD1	ABHD1	ABHD1	IVD	SARDH	ALDH5A1	ABHD1	PCYOX1	QDPR	QDPR
SARDH	SARDH	SARDH	ACOX2	SLC16A2	ACADSB	PDK2	SLC16A2	HOGA1	HOGA1
ACACB	ACACB	ACACB	HOGA1	IVD	PDK2	GSTA1	HOGA1	GLYATL1	GLS2
SULT1E1	XYLB	XYLB	ACOX1	QDPR	SARDH	ACACB	SLC16A10	GLS2	HAAO
B Genes that appear in top ten TCMR archetype GO terms (enriched in TCMR AA phenotype) N=765									
Term 1: T cell activation	Term 2: lymphocyte differentiation	Term 3: regulation of T cell activation	Term 4: mononuclear cell differentiation	Term 5: leukocyte cell- cell adhesion	Term 6: regulation of leukocyte cell- cell adhesion	Term 7: T cell differentiation	Term 8: positive regulation of leukocyte cell- cell adhesion	Term 9: positive regulation of T cell activation	Term 10: positive regulation of leukocyte activation
IL23A	IL23A	IL23A	IL23A	IL23A	IL23A	IL23A	IL23A	IL23A	TRBC1
CD3D	CD3D	CD2	CD3D	CD27	CD27	CD3D	CD27	CD27	TRBC2
CD2	CD2	CD27	CD2	LCK	LCK	CD2	LCK	LCK	IL23A
CD27	CD27	LCK	CD27	CD6	CD6	CD27	CD6	CD6	CD2
CD8A	CD8A	CD6	CD8A	RASGRP1	RASGRP1	CD8A	RASGRP1	RASGRP1	CD27
LCK	LCK	RASGRP1	LCK	HLA-DRA	HLA-DRA	LCK	HLA-DRA	HLA-DRA	LCK
ITK	ITK	HLA-DRA	ITK	TESPA1	TESPA1	ITK	TESPA1	TESPA1	CD6
CD6	THEMIS	TESPA1	THEMIS	CORO1A	CORO1A	THEMIS	CORO1A	CORO1A	RASGRP1
CD48	RASGRP1	CORO1A	RASGRP1	HLA-DPA1	HLA-DPA1	RASGRP1	HLA-DPA1	HLA-DPA1	HLA-DRA
THEMIS	HLA-DRA	HLA-DPA1	HLA-DRA	HLA-DPB1	HLA-DPB1	HLA-DRA	HLA-DPB1	HLA-DPB1	TESPA1
C Genes that appear in top ten NKRL GO terms (enriched in NKRL phenotype) N=765									
Term 1: T cell activation	Term 2: leukocyte mediated immunity	Term 3: regulation of immune effector process	Term 4: immune response- regulating cell surface receptor signaling pathway	Term 5: activation of immune response	Term 6: immune response- regulating signaling pathway	Term 7: negative regulation of immune system process	Term 8: leukocyte cell- cell adhesion	Term 9: immune response- activating cell surface receptor signaling pathway	Term 10: immune response- activating signal transduction
CD160	SH2D1B	SH2D1B	TRDC	TRDC	TRDC	CD160	CD160	TRDC	TRDC
XCL1	TRDC	CD160	CD160	CD160	CD160	CX3CR1	CX3CR1	CD160	CD160
EOMES	CD160	CX3CR1	KLRD1	KLRD1	KLRD1	KLRD1	XCL1	KLRD1	KLRD1
TBX21	PRF1	KLRD1	CD247	CD247	CD247	XCL1	TBX21	CD247	CD247
KLRC4-KLRK1	CX3CR1	XCL1	KLRC1	CD5L	KLRC1	TBX21	KLRC4-KLRK1	FCRL3	FCRL3
PDCD1LG2	KLRD1	NCR1	FCRL3	FCRL3	FCRL3	KLRC4-KLRK1	PDCD1LG2	PRKCB	PRKCB
KLRC1	XCL1	TBX21	PRKCB	PRKCB	PRKCB	LST1	RUNX3	LCP2	LCP2
RUNX3	NCR1	KLRC4-KLRK1	LCP2	LCP2	LCP2	PDCD1LG2	CCL5	PVRIG	PVRIG
CCL5	GZMB	CD5L	PVRIG	PVRIG	PVRIG	CST7	RAC2	PRKCH	PRKCH
RAC2	TBX21	KLRC1	PRKCH	PRKCH	PRKCH	KLRC1	ITGAL	BTN3A1	BTN3A1
D Genes that appear in top nine Injury GO terms (enriched in injury phenotype) N=765									
Term 1: extrinsic apoptotic signaling pathway	Term 2: regulation of apoptotic signaling pathway	Term 3: negative regulation of apoptotic signaling pathway	Term 4: regulation of extrinsic apoptotic signaling pathway	Term 5: negative regulation of extrinsic apoptotic signaling pathway	Term 6: response to oxidative stress	Term 7: response to endoplasmic reticulum stress	Term 8: biological process involved in symbiotic interaction	Term 9: actin filament bundle organization	
TMBIM1	TMBIM1	TMBIM1	TMBIM1	TMBIM1	GPX3	HYOU1	PVR	TNFAIP1	
KRT8	ENO1	ENO1	LMNA	LMNA	SP1	TNFRSF10B	TMPRSS2	SDC4	
LMNA	LMNA	LMNA	YAP1	YAP1	SIRPA	BCL2L1	SP1	ARHGEF5	
YAP1	YAP1	YAP1	TNFRSF12A	FAIM	GSR	ATP2A2	SCARB2	F11R	
TNFRSF12A	TNFRSF12A	FAIM	FAIM	BCL2L1	ITGA6	HMOX2	VAPB	NEDD9	
FAIM	FAIM	HYOU1	BCL2L1	ITGA6	MCL1	C19orf12	EDEM1	BCL2L1	
KRT18	HYOU1	SLC35F6	SLC35F6	MCL1	THBS1	ATP2A2	UBQLN1	RHOC	
TNFRSF10B	SLC35F6	BCL2L1	BCL2L1	ATP2A2	ATP2A2	ATP2A2	SLC3A2	SHTN1	
BCL2L1	BCL2L1	ITGA6	ITGA6	ATP2A2	ATP2A2	ATP2A2	TBC1D20	MIR21	
ITGA6	ITGA6	MCL1	ATF3	ATP2A2	ATP2A2	ATP2A2	CALR	F11R	

Note. Genes enriched per term are sorted by spearman correlation coefficient (descending). All gene lists per term were truncated to include only the top 10 terms per this sorting.
*Only 9 terms were found for the top genes in the Injury archetype group.

FIGURE 6. Genes enriched in each of the top 10 GO terms found for the NR (A), TCMR (B), NKRL (C), and Injury phenotypes (D; only 9 terms were found for Injury). Each gene is colored according to its most prominent expression in a cell panel. AA, archetypal analysis; GO, gene ontology; NKRL, natural killer cell–enriched rejection-like; NR, no rejection; TCMR, T cell–mediated rejection.

effects but not in the long term.^{73,74} We will need long-term experience with the NKRL state before concluding that it is benign.

The frequency of archetypal TCMR biopsies rose and peaked before becoming rare after 3 y posttransplant, similar to the distribution of molecular TCMR in kidney

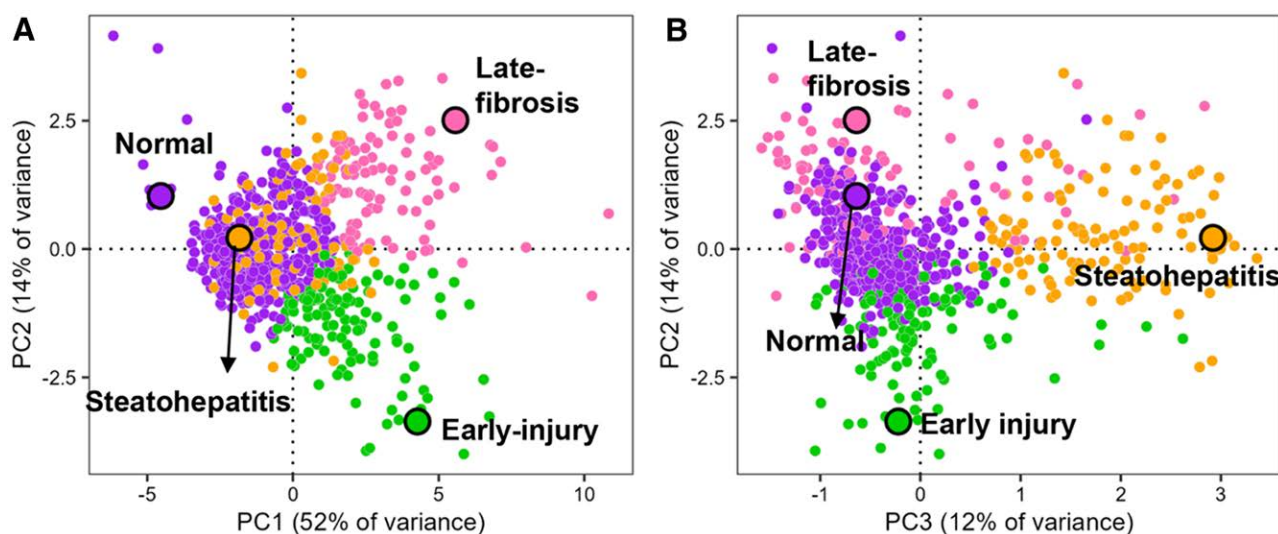


FIGURE 7. The rederived archetypal and PC analyses for liver injury using AMAT1, QCMMAT, DAMP, IGT, IRITD3, and IRID5 plus the steatohepatitis and fibrosis classifiers as input. Normal, Early-injury, Steatohepatitis, and Late-fibrosis groups are shown in PC2 vs PC1 (A), and PC2 vs PC3 (B). AMAT1, alternative macrophage activation-associated transcripts; DAMP, damage-associated molecular pattern transcripts; IGT, immunoglobulin transcripts; IRITD3, injury and repair-induced transcripts-day 3; IRID5, injury and repair-induced transcripts-day 5; PC, principal component; QCMMAT, quantitative constitutive macrophage-associated transcripts.

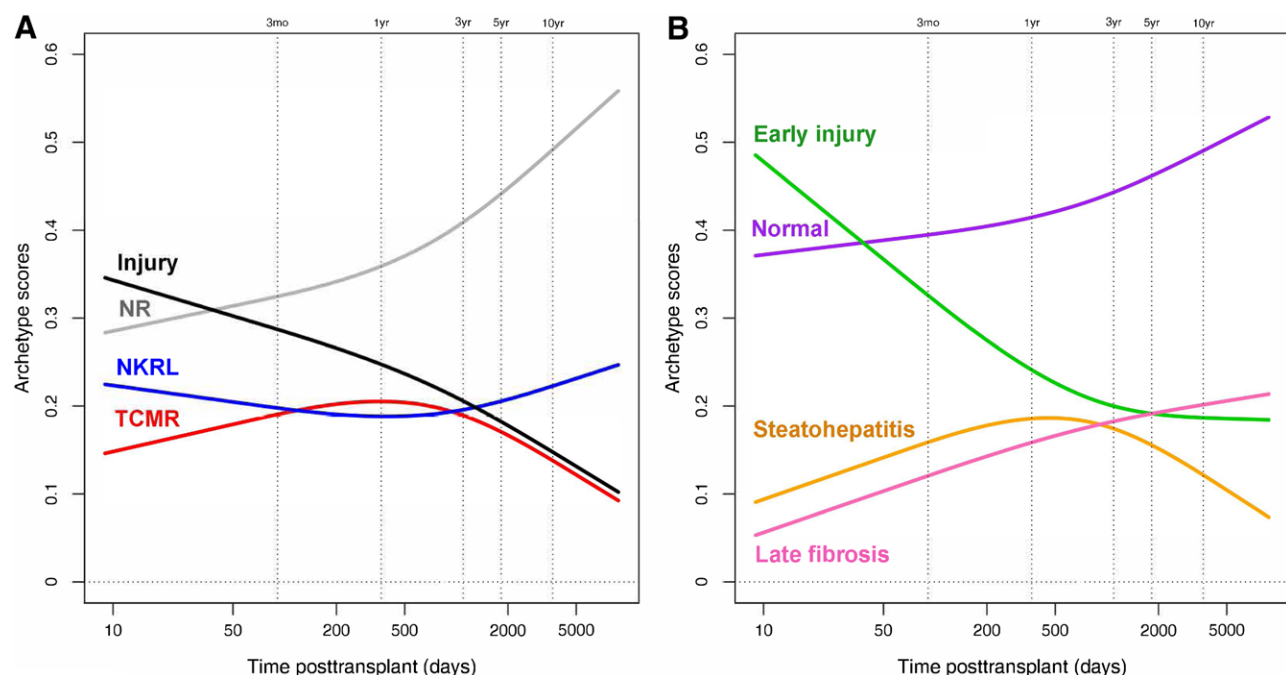


FIGURE 8. Time course visualization for each rejection archetype score as restricted cubic splines. Although no rejection increases over time, NKRL states decrease toward 500 d before a slight increase. TCMR rises to peak around 400 d before declining. Injury declines steadily over time. NKRL, natural killer cell–enriched rejection-like; TCMR, T cell–mediated rejection.

and heart transplants and suggesting regulatory mechanisms like immunologic checkpoints. Molecular TCMR was associated with the typical histologic lesions and was diagnosed in 125 of 765 biopsies (16%), similar to reports of clinical TCMR in the liver transplant population.^{75,76} Our TCMR group was also associated with histologic inflammation, that is, portal inflammation ($P = 1.4E-9$), fibrosis (mural fibrosis $P = 0.04$, molecular fibrosis by archetype assignment, and the fibrosis classifier $P < 2.2E-16$), and molecular rejection genes, that is, ITK and CD8A, similar to literature findings by Feng et al.²¹ Some

molecular TCMR occurred after the first year, recalling long-standing concerns about the significance of late TCMR in liver transplants.⁷⁷ Molecular TCMR was associated with increased expression of injury-associated transcript sets, with Early-injury and Late fibrosis injury archetypes, and with biochemical abnormalities. Given the implications of histologic TCMR for graft function, survival, and potential development of chronic rejection,^{78,79} further definition of molecular TCMR, its consequences, and implications for immunosuppressive management will be an important future focus.

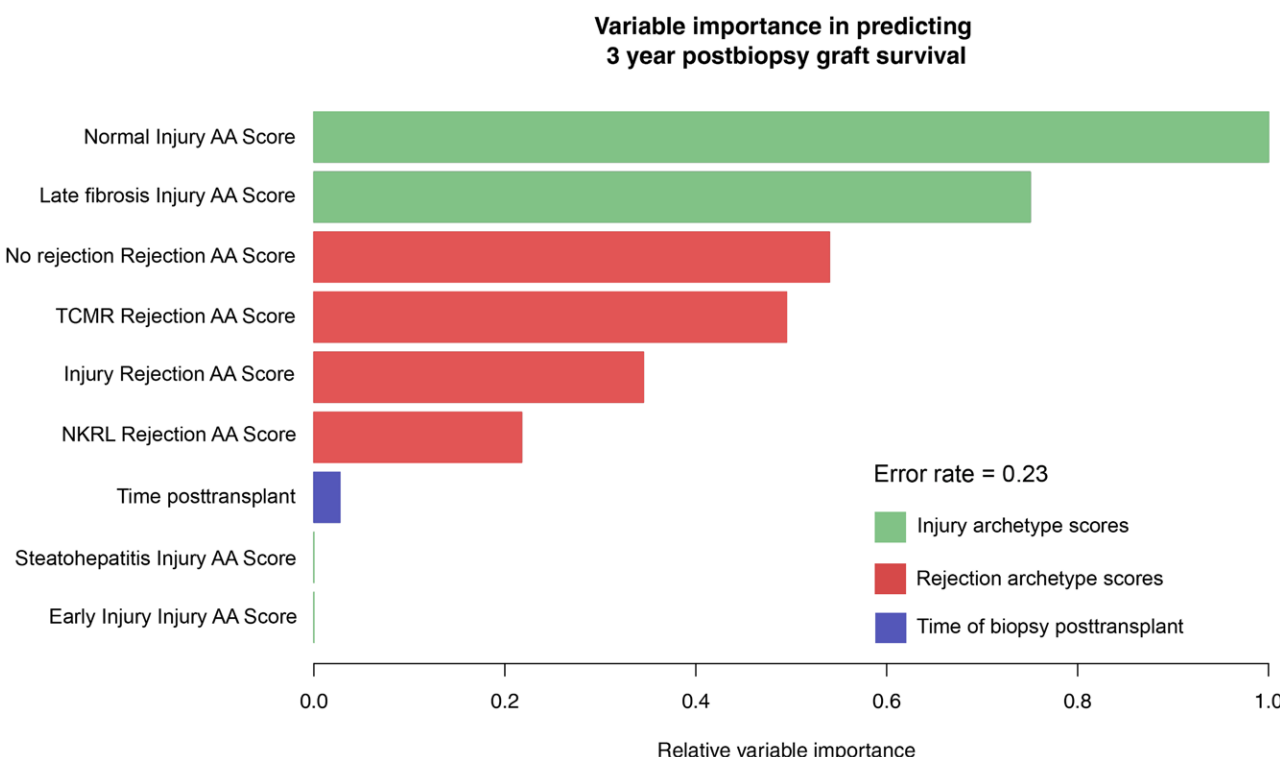


FIGURE 9. Random forest relative variable importance for predicting 3-y graft survival amongst rejection (pink) and injury (green) archetype scores plus time of biopsy posttransplant (blue). Events were death-censored. AA, archetypal analysis; NKRL, natural killer cell–enriched rejection-like; TCMR, T cell–mediated rejection.

Although NK cells are associated with long-term damage in AMR in kidney and heart transplants, and anti-CD38 monoclonal felzartamab suppresses NK cells and AMR activity in the kidney,³⁸ other roles of NK cells in liver transplants are possible. The liver differs from the kidney and heart in that NK cells constitute >40% of the hepatic lymphocyte population.⁸⁰ Moreover, a large proportion of hepatic NK cells are CD56^{bright}CD16⁻ liver-resident NK cells (ie, noncirculating).³⁹ There is growing literature supporting the concept of liver-resident CD56^{bright}CD16⁻ cells operating as a control to limit the activity of infiltrating T cells against the graft.^{39–42} In this hypothesis, the donor hepatic NK cells are capable of killing recipient immune cells recruited to the graft tissue (ie, activated T cells, recipient immature dendritic cells).⁴¹ NK cells may be associated with T-cell exhaustion, resulting in good short-term outcomes but late allograft injury—an effect seen in murine liver transplant tolerance studies.⁸¹ Our alternative hypothesis is that NKRL represents a phenotype enriched with liver-resident NK cells potentially capable of direct lysis of allogenic infiltrating T cells.³⁹ Normal biochemistry, increased expression of NK cell-associated transcripts even above the NR biopsies, the converse time scale for NKRL versus TCMR, and increased expression of genes differentially expressed by liver-resident (donor) NK cells⁸² with the NKRL archetype (eg, CD160, IL2RB, SH2D1A) all support ongoing exploration of this hypothesis. Expression of FCGR3A (expressed more strongly by circulating CD56^{dim}CD16⁺ recipient-derived NK cells)⁸² in NKRL state was also lower compared with TCMR, suggesting a lower activation of CD16⁺ NK cells in NKRL biopsies. Moreover, although we had too little follow-up data to infer better outcomes of liver transplants with

NKRL, the NKRL state in lung transplant biopsies had 3-y graft loss comparable with NR.⁴³ It would be of great interest to examine the diversity of CD56 cells (ie, CD56^{bright}CD16⁻ versus CD56^{dim}CD16⁺) in NKRL biopsies by either immunohistochemistry or single-cell transcriptomics to reveal diagnostic histologic features of the NKRL state.

Comparison of the present genome-wide molecular findings in liver transplants to the results of genome-wide analyses of kidney, heart, and lung transplants in the MMDx system^{43,49,69,74,83,84} confirms the unique properties of liver transplants. Compared with kidneys,^{69,74,83,85–87} hearts,^{71,84,88} and lungs,^{43,89,90} the states that we designated as the NR and normal archetypes in the liver progressively increase over time as early transplantation injury resolves and become dominant after 1 y posttransplant. Liver transplants rarely develop late atrophy fibrosis molecular phenotypes, which are common in late kidney and heart transplants and are much more stable than lungs.^{43,89} The unique properties of liver transplants stand out even as viewed through the biopsy perspective, which overrepresents abnormalities (because the best livers are not biopsied).

The relationship of the NKRL-like state to other clinical or histologic definitions and features of Banff-defined AMR in liver transplants remains an open question, as most of the INTERLIVER centers did not identify definite AMR cases in their histologic reports, and the recent review of AMR states that “the role of AMR in liver transplantation remains controversial.”¹ The relationship of the NKRL state to Banff AMR remains unknown. However, the resolution of these questions is important for our approach to immunosuppression management.

Ongoing analyses must elucidate whether NKRL is a form of hepatic AMR or a separate NK-mediated phenotype potentially with regulatory effects, and how clinicians should interpret this state. Limitations to this study include those common to cross-sectional biopsy studies: we can only apply our findings to transplants that have been biopsied, follow-up time remains limited, and treatment information was not suitable for incorporation at this stage of the study. The limited availability of clear histologic rejection diagnoses has also impacted our analyses and caused us to focus on comparing the molecular rejection states to the available histologic and clinical features. Nevertheless, this study identified an NKRL state in liver transplant biopsies that is relatively well-tolerated short term and unrelated to histology classifications and a separate TCMR phenotype consistent in many ways with histologic TCMR. Our focus going forward will be on establishing the clinical significance of the NKRL states and their relationship to the host alloimmune response.

REFERENCES

1. Lucey MR, Furuya KN, Foley DP. Liver transplantation. *N Engl J Med*. 2023;389:1888–1900.
2. McCaughan GW, Gorrell MD, Bishop GA, et al. Molecular pathogenesis of liver disease: an approach to hepatic inflammation, cirrhosis and liver transplant tolerance. *Immunol Rev*. 2000;174:172–191.
3. Neuberger J. An update on liver transplantation: a critical review. *J Autoimmun*. 2016;66:51–59.
4. Zarrinpar A, Busuttil RW. Liver transplantation: past, present and future. *Nat Rev Gastroenterol Hepatol*. 2013;10:434–440.
5. Wadstrom J, Ericzon BG, Halloran PF, et al. Advancing transplantation: new questions, new possibilities in kidney and liver transplantation. *Transplantation*. 2017;101(Suppl 2S):S1–S41.
6. Demetris AJ, Bellamy C, Hubscher SG, et al. 2016 Comprehensive update of the Banff Working Group on liver allograft pathology: introduction of antibody-mediated rejection. *Am J Transplant*. 2016;16:2816–2835.
7. Fisher LR, Henley KS, Lucey MR. Acute cellular rejection after liver transplantation: variability, morbidity, and mortality. *Liver Transpl Surg*. 1995;1:10–15.
8. Regev A, Molina E, Moura R, et al. Reliability of histopathologic assessment for the differentiation of recurrent hepatitis C from acute rejection after liver transplantation. *Liver Transpl*. 2004;10:1233–1239.
9. Younossi ZM, Boparai N, Gramlich T, et al. Agreement in pathologic interpretation of liver biopsy specimens in posttransplant hepatitis C infection. *Arch Pathol Lab Med*. 1999;123:143–145.
10. Pournik O, Alavian SM, Ghalichi L, et al. Inter-observer and intra-observer agreement in pathological evaluation of non-alcoholic fatty liver disease suspected liver biopsies. *Hepat Mon*. 2014;14:e15167.
11. Wiesner RH. Is hepatic histology the true gold standard in diagnosing acute hepatic allograft rejection? *Liver Transpl Surg*. 1996;2:165–167.
12. Horvath B, Allende D, Xie H, et al. Interobserver variability in scoring liver biopsies with a diagnosis of alcoholic hepatitis. *Alcohol Clin Exp Res*. 2017;41:1568–1573.
13. Montano-Loza AJ, Rodriguez-Peralvarez ML, Pageaux GP, et al. Liver transplantation immunology: immunosuppression, rejection, and immunomodulation. *J Hepatol*. 2023;78:1199–1215.
14. Clavien PA, Muller X, de Oliveira ML, et al. Can immunosuppression be stopped after liver transplantation? *Lancet Gastroenterol Hepatol*. 2017;2:531–537.
15. Ascha MS, Ascha ML, Hanouneh IA. Management of immunosuppressant agents following liver transplantation: less is more. *World J Hepatol*. 2016;8:148–161.
16. Moini M, Schilsky ML, Tichy EM. Review on immunosuppression in liver transplantation. *World J Hepatol*. 2015;7:1355–1368.
17. Lerut J, Sanchez-Fueyo A. An appraisal of tolerance in liver transplantation. *Am J Transplant*. 2006;6:1774–1780.
18. Terasaki PI. Tolerogenic mechanisms in liver transplantation. *SOJ Immunol*. 2015;3:01–13.
19. Mofrad P, Contos MJ, Haque M, et al. Clinical and histologic spectrum of nonalcoholic fatty liver disease associated with normal ALT values. *Hepatology*. 2003;37:1286–1292.
20. Sorrentino P, Tarantino G, Conca P, et al. Silent non-alcoholic fatty liver disease—a clinical-histological study. *J Hepatol*. 2004;41:751–757.
21. Feng S, Bucuvalas JC, Demetris AJ, et al. Evidence of chronic allograft injury in liver biopsies from long-term pediatric recipients of liver transplants. *Gastroenterology*. 2018;155:1838–1851.e7.
22. Lee M. Antibody-mediated rejection after liver transplant. *Gastroenterol Clin North Am*. 2017;46:297–309.
23. Taner T, Stegall MD, Heimbach JK. Antibody-mediated rejection in liver transplantation: current controversies and future directions. *Liver Transpl*. 2014;20:514–527.
24. Dao M, Habes D, Taupin JL, et al. Morphological characterization of chronic antibody-mediated rejection in ABO-identical or ABO-compatible pediatric liver graft recipients. *Liver Transpl*. 2018;24:897–907.
25. Levitsky J, Feng S. Tolerance in clinical liver transplantation. *Hum Immunol*. 2018;79:283–287.
26. Thomson AW, Knolle PA. Antigen-presenting cell function in the tolerogenic liver environment. *Nat Rev Immunol*. 2010;10:753–766.
27. Vionnet J, Sanchez-Fueyo A. Biomarkers of immune tolerance in liver transplantation. *Hum Immunol*. 2018;79:388–394.
28. Mastoridis S, Martinez-Llordella M, Sanchez-Fueyo A. Emergent transcriptomic technologies and their role in the discovery of biomarkers of liver transplant tolerance. *Front Immunol*. 2015;6:304.
29. Savage TM, Shonts BA, Lau S, et al. Deletion of donor-reactive T cell clones after human liver transplant. *Am J Transplant*. 2020;20:538–545.
30. Madill-Thomsen K, Abouljoud M, Bhati C, et al. The molecular diagnosis of rejection in liver transplant biopsies: first results of the INTERLIVER study. *Am J Transplant*. 2020;20:2156–2172.
31. Nakamura T, Shirouzu T. Antibody-mediated rejection and recurrent primary disease: two main obstacles in abdominal kidney, liver, and pancreas transplants. *J Clin Med*. 2021;10:5417.
32. Hubscher SG. Antibody-mediated rejection in the liver allograft. *Curr Opin Organ Transplant*. 2012;17:280–286.
33. Montgomery RA, Loupy A, Segev DL. Antibody-mediated rejection: new approaches in prevention and management. *Am J Transplant*. 2018;18(Suppl 3):3–17.
34. Ballellas C, Llado L, Serrano T, et al. Sinusoidal obstruction syndrome as a manifestation of acute antibody-mediated rejection after liver transplantation. *Am J Transplant*. 2021;21:3775–3779.
35. Lee BT, Fiel MI, Schiano TD. Antibody-mediated rejection of the liver allograft: an update and a clinico-pathological perspective. *J Hepatol*. 2021;75:1203–1216.
36. O’Leary JG, Kaneko H, Demetris AJ, et al. Antibody-mediated rejection as a contributor to previously unexplained early liver allograft loss. *Liver Transpl*. 2014;20:218–227.
37. Madill-Thomsen KS, Abouljoud M, Bhati C, et al. The molecular phenotypes of injury, steatohepatitis, and fibrosis in liver transplant biopsies in the INTERLIVER study. *Am J Transplant*. 2022;22:909–926.
38. Mayer KA, Schrezenmeier E, Diebold M, et al. A randomized phase 2 trial of felzartamab in antibody-mediated rejection. *N Engl J Med*. 2024;391:122–132.
39. Jameson G, Harmon C, Santiago RM, et al. Human hepatic CD56(bright) NK cells display a tissue-resident transcriptional profile and enhanced ability to kill allogenic CD8(+) T cells. *Front Immunol*. 2022;13:921212.
40. Halma J, Pierce S, McLennan R, et al. Natural killer cells in liver transplantation: can we harness the power of the immune checkpoint to promote tolerance? *Clin Transl Sci*. 2022;15:1091–1103.
41. Jiang Y, Que W, Zhu P, et al. The role of diverse liver cells in liver transplantation tolerance. *Front Immunol*. 2020;11:1203.
42. Harmon C, Sanchez-Fueyo A, O’Farrelly C, et al. Natural killer cells and liver transplantation: orchestrators of rejection or tolerance? *Am J Transplant*. 2016;16:751–757.
43. Gauthier PT, Mackova M, Hirji A, et al. Defining a natural killer cell-enriched molecular rejection-like state in lung transplant transbronchial biopsies. *Am J Transplant*. 2023;23:1922–1938.
44. Halloran PF, Reeve J, Akalin E, et al. Real time central assessment of kidney transplant indication biopsies by microarrays: the INTERCOMEX study. *Am J Transplant*. 2017;17:2851–2862.
45. Martinez-Llordella M, Puig-Pey I, Orlando G, et al. Multiparameter immune profiling of operational tolerance in liver transplantation. *Am J Transplant*. 2007;7:309–319.

46. Bonaccorsi-Riani E, Pennycuick A, Londono MC, et al. Molecular characterization of acute cellular rejection occurring during intentional immunosuppression withdrawal in liver transplantation. *Am J Transplant.* 2016;16:484–496.
47. ATAGC. Gene lists. Available at <https://www.ualberta.ca/medicine/institutes-centres-groups/atagc/research/gene-lists>. Accessed April 4, 2022.
48. Reeve J, Bohmig GA, Eskandary F, et al; MMDx-Kidney Study Group. Assessing rejection-related disease in kidney transplant biopsies based on archetypal analysis of molecular phenotypes. *JCI Insight.* 2017;2:e94197.
49. Reeve J, Kim DH, Crespo-Leiro MG, et al. Molecular diagnosis of rejection phenotypes in 889 heart transplant biopsies: the INTERHEART study. *J Heart Lung Transplant.* 2018;37:S27–S27.
50. Eugster MJA, Leisch F. From spider-man to hero—archetypal analysis in R. *J Statist Software.* 2009;30:1–23.
51. Famulski KS, Sis B, Billesberger L, et al. Interferon-gamma and donor MHC class I control alternative macrophage activation and activin expression in rejecting kidney allografts: a shift in the Th1-Th2 paradigm. *Am J Transplant.* 2008;8:547–556.
52. Land WG, Agostinis P, Gasser S, et al. Transplantation and damage-associated molecular patterns (DAMPs). *Am J Transplant.* 2016;16:3338–3361.
53. Einecke G, Reeve J, Mengel M, et al. Expression of B cell and immunoglobulin transcripts is a feature of inflammation in late allografts. *Am J Transplant.* 2008;8:1434–1443.
54. Famulski KS, Broderick G, Einecke G, et al. Transcriptome analysis reveals heterogeneity in the injury response of kidney transplants. *Am J Transplant.* 2007;7:2483–2495.
55. Famulski KS, Einecke G, Sis B, et al. Defining the canonical form of T-cell-mediated rejection in human kidney transplants. *Am J Transplant.* 2010;10:810–820.
56. (2019) RCT. R: A language and environment for statistical computing. Available at <http://www.r-project.org/>. Accessed January 7, 2022.
57. Lê S, Josse J, Husson F. FactoMineR: AnRPackage for Multivariate Analysis. *J Statist Software.* 2008;25:18.
58. Wood SN. *Generalized Additive Models*. 2nd ed. Boca Raton, FL: Chapman and Hall/CRC; 2017.
59. Venner JM, Famulski KS, Badr D, et al. Molecular landscape of T cell-mediated rejection in human kidney transplants: prominence of CTLA4 and PD ligands. *Am J Transplant.* 2014;14:2565–2576.
60. Uhlen M, Fagerberg L, Hallstrom BM, et al. Proteomics. Tissue-based map of the human proteome. *Science.* 2015;347:1260419.
61. Harrell FE Jr, Dupont C. Hmisc: Harrell miscellaneous. R package version 4.3-0. Available at <https://CRAN.R-project.org/package=Hmisc>. Accessed January 7, 2022.
62. Ishwaran H, Kogalur UB. Fast Unified Random Forests for Survival, Regression, and Classification (RF-SRC). R package version 302. Available at <https://cran.r-project.org/web/packages/randomForestSRC/index.html>. Accessed July 5, 2022.
63. Ritchie ME, Phipson B, Wu D, et al. limma powers differential expression analyses for RNA-sequencing and microarray studies. *Nucleic Acids Res.* 2015;43:e47.
64. Smythe GK. limma: linear models for microarray data. In: Gentleman RHW, Carey VJ, Irizarry RA, et al, ed. *Bioinformatics and Computational Biology Solutions using R and Bioconductor*. Springer; 2005:398–420.
65. Wobbrock JFL, Gergle D, Higgins J. The aligned rank transform for nonparametric factorial analyses using only ANOVA procedures. In: Proceedings of the ACM Conference on Human Factors in Computing Systems (CHI '11), May 7–12, 2011. Vancouver, BC, Canada: ACM Press; 2011;143–146. Available at <https://depts.washington.edu/acelab/proj/art/>. Accessed July 3, 2022.
66. Kay MEL, Higgins J, Wobbrock J. ARTTool: aligned rank transform for nonparametric factorial ANOVAs, R package version 0.111. Available at <https://github.com/mjskay/ARTTool>. Accessed July 2, 2022.
67. Yu G, Wang LG, Han Y, et al. clusterProfiler: an R package for comparing biological themes among gene clusters. *OMICS.* 2012;16:284–287.
68. Halloran PF, Madill-Thomsen KS, Reeve J. The molecular phenotype of kidney transplants: insights from the MMDx project. *Transplantation.* 2024;108:45–71.
69. Madill-Thomsen KS, Bohmig GA, Bromberg J, et al; the INTERCOMEX Investigators. Relating molecular T cell-mediated rejection activity in kidney transplant biopsies to time and to histologic tubulitis and atrophy-fibrosis. *Transplantation.* 2023;107:1102–1114.
70. Halloran PF, Madill-Thomsen K, Aliabadi-Zuckermann AZ, et al. Redefining the molecular rejection states in 3230 heart transplant biopsies: relationships to parenchymal injury and graft survival. *Am J Transplant.* 2024;S1600-6135:00241–00247.
71. Madill-Thomsen KS, Reeve J, Aliabadi-Zuckermann A, et al. Assessing the relationship between molecular rejection and parenchymal injury in heart transplant biopsies. *Transplantation.* 2022;106:2205–2216.
72. Einecke G, Reeve J, Gupta G, et al; INTERCOMEX Investigators. Factors associated with kidney graft survival in pure antibody-mediated rejection at the time of indication biopsy: importance of parenchymal injury but not disease activity. *Am J Transplant.* 2021;21:1391–1401.
73. Halloran P, Madill-Thomsen K, Gauthier P, et al. Reclassifying rejection in 3258 heart transplant biopsies using optimized algorithms. *Am J Transplant.* 2023;23:S424.
74. Halloran P, Reeve J, Madill-Thomsen K, et al. The spectrum of molecular rejection in the prevalent kidney transplant population: a new analysis of 5087 biopsies. *Am J Transplant.* 2023;23:S371–S372.
75. Rodriguez-Peralvarez M, Rico-Juri JM, Tsochatzis E, et al. Biopsy-proven acute cellular rejection as an efficacy endpoint of randomized trials in liver transplantation: a systematic review and critical appraisal. *Transpl Int.* 2016;29:961–973.
76. Choudhary NS, Saigal S, Bansal RK, et al. Acute and chronic rejection after liver transplantation: what a clinician needs to know. *J Clin Exp Hepatol.* 2017;7:358–366.
77. Jadlowiec CC, Morgan PE, Nehra AK, et al. Not all cellular rejections are the same: differences in early and late hepatic allograft rejection. *Liver Transpl.* 2019;25:425–435.
78. Thomson M, Lake JR. CAQ Corner: immune-mediated complications. *Liver Transpl.* 2023;29:885–893.
79. Levitsky J, Goldberg D, Smith AR, et al. Acute rejection increases risk of graft failure and death in recent liver transplant recipients. *Clin Gastroenterol Hepatol.* 2017;15:584–593.e2.
80. Harmon C, Robinson MW, Fahey R, et al. Tissue-resident Eomes(hi) T-bet(lo) CD56(bright) NK cells with reduced proinflammatory potential are enriched in the adult human liver. *Eur J Immunol.* 2016;46:2111–2120.
81. Good CR, Aznar MA, Kuramitsu S, et al. An NK-like CAR T cell transition in CAR T cell dysfunction. *Cell.* 2021;184:6081–6100.e26.
82. Jameson G, Robinson MW. Insights into human intrahepatic NK cell function from single cell RNA sequencing datasets. *Front Immunol.* 2021;12:649311.
83. Madill-Thomsen KS, Bohmig GA, Bromberg J, et al; INTERCOMEX Investigators. Donor-specific antibody is associated with increased expression of rejection transcripts in renal transplant biopsies classified as no rejection. *J Am Soc Nephrol.* 2021;32:2743–2758.
84. Halloran PF, Madill-Thomsen K, Mackova M, et al. Molecular states associated with dysfunction and graft loss in heart transplants. *J Heart Lung Transplant.* 2024;43:508–518.
85. Halloran PF, Madill-Thomsen KS, Pon S, et al; INTERCOMEX Investigators. Molecular diagnosis of ABMR with or without donor-specific antibody in kidney transplant biopsies: differences in timing and intensity but similar mechanisms and outcomes. *Am J Transplant.* 2022;22:1976–1991.
86. Halloran PF, Bohmig GA, Bromberg J, et al; INTERCOMEX Investigators. Archetypal analysis of injury in kidney transplant biopsies identifies two classes of early AKI. *Front Med (Lausanne).* 2022;9:817324.
87. Reeve J, Bohmig GA, Eskandary F, et al; INTERCOMEX MMDx-Kidney Study Group. Generating automated kidney transplant biopsy reports combining molecular measurements with ensembles of machine learning classifiers. *Am J Transplant.* 2019;19:2719–2731.
88. Parkes MD, Aliabadi AZ, Cadeiras M, et al. An integrated molecular diagnostic report for heart transplant biopsies using an ensemble of diagnostic algorithms. *J Heart Lung Transplant.* 2019;38:636–646.
89. Parkes MD, Halloran K, Hirji A, et al. Transcripts associated with chronic lung allograft dysfunction in transbronchial biopsies of lung transplants. *Am J Transplant.* 2022;22:1054–1072.
90. Halloran KM, Parkes MD, Chang J, et al. Molecular assessment of rejection and injury in lung transplant biopsies. *J Heart Lung Transplant.* 2019;38:504–513.